Indole-3-carbinol Inhibits Protein Kinase B/Akt and Induces Apoptosis in the Human Breast Tumor Cell Line MDA MB468 but not in the Nontumorigenic HBL100 Line[1]

Lynne M. Howells, Barbara Gallacher-Horley, Catherine E. Houghton, Margaret M. Manson, and E. Ann Hudson[2]

Cancer Biomarkers and Prevention Group, Biocentre, University of Leicester, Leicester LE1 7RH [L. M. H., B. G-H., M. M. M., E. A. H.], and Medical Research Council Toxicology Unit, University of Leicester, Leicester LE1 9HN [C. E. H.], United Kingdom

Abstract

We have identified a new target for the chemopreventive dietary agent indole-3-carbinol (I3C) in the antiapoptotic signaling pathway involving phosphatidylinositol 3′-kinase and protein kinase B (PKB)/Akt. I3C inhibited phosphorylation and activation of PKB in the tumor-derived breast cell line MDA MB468, but not in the immortalized breast line HBL100. We propose that this cell type-specific response to I3C contributes to the differential induction of apoptosis and sensitivity to growth inhibition of the two cell lines (approximate IC_{50} = 30 μM for the MDA MB468 line, compared with 120 μM for the HBL100 line). I3C only induced apoptosis in the MDA MB468 cell line, but at higher doses, it increased necrosis in the HBL100 line. The tumor cell line was also markedly less able to recover when I3C was removed from the culture medium. Downstream of PKB, I3C decreased nuclear factor κB DNA binding, independently of an effect on IκB kinase, in the MDA MB468 cell line only. The tumor suppressor PTEN, which prevents phosphorylation and activation of PKB, was expressed in HBL100 cells but was not detected in MDA MB468 cells. In corroboration of the results obtained with the breast cell lines, I3C decreased phospho-PKB levels and induced apoptosis in the prostate cell line LNCaP, which expresses very low levels of PTEN, but did not do so in PTEN-positive DU145 cells. I3C did not affect PTEN levels in any cell line. This is the first study to report a differential mechanistic response of tumor-derived and nontumorigenic cell lines and of PTEN high- and low-expressing cells to I3C and indicates a promising chemopreventive role for I3C against estrogen receptor-α-negative, aggressive-phenotype breast tumors.

Introduction

I3C,[3] a microconstituent derived from cruciferous vegetables such as broccoli and Brussels sprouts, has been shown to exert antitumor and chemopreventive activity against chemically induced tumors at a variety of sites in rodent models (1–4). Two Phase I clinical trials of I3C with promising results have been reported, featuring patients with recurrent respiratory papillomatosis or cervical intraepithelial neoplasia (5, 6). I3C has also been the subject of a breast cancer prevention dose-finding pilot study (7) and has been shown to act cooperatively with tamoxifen *in vitro* (8). There is little in the literature regarding the physiological levels of I3C achievable *in vivo*, but one study reported I3C equivalents of 120 μM in liver after a single oral administration of 50 mg/kg [^{14}C]I3C in rats (9). The mechanism by which I3C exerts its chemoprotective effect has not been fully elucidated, although a number of potential cellular targets have been implicated. We showed previously that I3C not only acted to prevent tumor development when given before the carcinogen in an aflatoxin B_1 hepatocarcinogenesis model but also completely inhibited tumor formation when added to the diet from 6 weeks postinitiation (1). The blocking activity of I3C has been well characterized in terms of modulation of phase I and II drug-metabolizing enzymes, leading to the rapid excretion of the carcinogen and prevention of DNA adduct formation (10–17).

The mechanism by which I3C exerts its tumor-suppressing activity is likely to involve modulation of cell signaling pathways resulting in inhibition of cell proliferation or induction of apoptosis (reviewed in Refs. 18 and 19). In the long-term feeding study mentioned above (1), we showed that after 13 weeks, in rats receiving oral I3C, liver activities of both total tyrosine kinase and ornithine decarboxylase were significantly decreased compared with those in rats not receiving the agent. I3C has also been shown to inhibit total tyrosine kinase activity *in vitro* (20), but little is known about its effect on specific kinases of cell signaling pathways. Cover *et al.* (21) showed that in MCF7 and MDA MB231 breast tumor cell lines, I3C caused G_0-G_1 cell cycle arrest, which was accompanied by a down-regulation of cyclin-dependent kinase 6, decreased retinoblastoma protein phosphorylation, and an increase in $p21^{WAF1}$ and p27. There is also evidence that I3C may exert its chemopreventive activity by induction of apoptosis. The compound caused a small but significant increase in apoptosis in the human breast tumor MDA MB231

Received 5/13/02; revised 9/6/02; accepted 10/3/02.
[1] Supported by the United Kingdom Medical Research Council. These data have been published in a preliminary form as an abstract (Ref. 46).
[2] To whom requests for reprints should be addressed, at Cancer Biomarkers and Prevention Group, Biocentre, University of Leicester, University Road, Leicester LE1 7RH, United Kingdom. Phone: 44-0-116-2231825; Fax: 44-0-116-2231840; E-mail: eah5@le.ac.uk.

[3] The abbreviations used are: I3C indole-3-carbinol; PKB, protein kinase B; PI3K, phosphatidylinositol 3′-kinase; NF-κB, nuclear factor κB; IκB, inhibitor of NF-κB; IKK, IκB kinase, PARP, poly(ADP-ribose) polymerase; GSK, glycogen synthase kinase; EMSA, electrophoretic mobility shift assay.

line and in the chemical- and oncogene-initiated 184-B5/BP and 184-B5/HER breast cell lines (22). Recently, Rahman *et al.* (23) showed induction of apoptosis in MDA MB435 cells and concluded that this was due to translocation of the proapoptotic molecule Bax to the mitochondria and an increase in the Bax:Bcl-2 ratio. However, an earlier study by Ge *et al.* (24) reported that I3C induced apoptosis in MCF7 cells via a p53- and Bax-independent pathway, although it should be noted that earlier time points were investigated in the latter study. In a previous study, Ge *et al.* (25) showed that 3,3′-diindolylmethane, an acid condensation product of I3C, induced apoptosis in MCF7 and T47D breast tumor cell lines and in Saos2 human osteosarcoma cells.

Many cell signaling pathways have been implicated in apoptosis, including components of the mitogen-activated protein kinase cascades and PKB (otherwise known as Akt) signaling pathways (reviewed in Ref. 26). Activation of c-Jun NH_2-terminal kinase and p38 kinase is generally associated with proapoptotic signaling (26–29), although there are some studies that implicate c-Jun in protection against stress-induced apoptosis (reviewed in Ref. 30). In contrast, activation of the extracellular signal-regulated kinases 1 and 2 and PKB (which lies downstream of PI3K) is associated with cell survival (26, 29, 31). Undoubtedly, it is the balance between pro- and antiapoptotic signaling under particular circumstances that ultimately determines the fate of a cell.

PKB has been shown to influence apoptosis via multiple downstream targets (32–34). It can phosphorylate and inactivate several proapoptotic proteins, including caspase 9 (35), members of the Forkhead family of transcription factors (Refs. 33 and 36 and the references therein), and Bad (both directly and via kinase $p65^{pak}$; Refs. 37–39). Phosphorylated Bad is sequestered by the cytosolic protein 14-3-3, thus preventing it from binding and inhibiting, the antiapoptotic proteins Bcl-2 and Bcl-xL (40). Bcl-2 itself has also been shown to be up-regulated by PKB via the transcription factor cAMP-responsive element-binding protein CREB (41). Activation of signaling via PKB also increases NF-κB-mediated cell survival (42, 43).

The phosphatase PTEN (PTEN/MMAC1/TEP1) tumor suppressor has also been implicated in the regulation of PKB and therefore in induction of apoptosis. Phosphorylation of PKB is required for full activation of the kinase (34). PTEN has been shown to dephosphorylate PI3K-generated phosphatidylinositol 3,4,5-trisphosphate molecules, the signaling intermediates required for activation of PKB (33, 44, 45).

In this study we compared the effects of I3C between the human breast tumor-derived cell line MDA MB468 and the normal tissue-derived HBL100 cell line. We investigated the induction of apoptosis in these cell lines and the role that inhibition of the PKB signaling pathway and of downstream effectors, including NF-κB, might play in this process. In agreement with our preliminary findings (46), our data indicated that I3C inhibited the phosphorylation and activity of PKB in the tumor cell line only and that this is likely to contribute to the induction of apoptosis and chemopreventive mechanism of action of I3C in these breast tumor cells. To confirm our results, we then extended the study to incorporate two prostate cancer cell lines, LNCaP and DU145.

Materials and Methods

Materials. I3C and okadaic acid were obtained from Sigma-Aldrich Company Ltd. (Poole, United Kingdom), and LY294002 was obtained from Calbiochem-Novabiochem (United Kingdom) Ltd. (Beeston, United Kingdom). The complete protease inhibitor mixture was purchased from Roche Diagnostics Ltd. (Lewes, United Kingdom). The IκBα substrate and anti-NF-κB p65 (C-20), anti-IKKα, and anti-Akt-1 antibodies were obtained from Santa Cruz Biotechnology (Santa Cruz, CA). Antibodies against PTEN and Akt (detects total PKBα, β, and γ, phosphorylation state independent), the two phosphorylation site-specific anti-phospho-Akt antibodies [anti-phospho-Akt (Ser 473) detects PKBα when phosphorylated at Ser-473 and detects PKBβ and PKBγ when phosphorylated at equivalent sites; and anti-phospho-Akt (Thr 308), which does not cross-react with the Ser-473 phosphorylation site], and the Akt kinase assay kit were from Cell Signaling Technology (Hitchin, United Kingdom). Antibody against Bcl-xL was purchased from BD Transduction Laboratories (Lexington, KY); the anti-Bcl-2 and Bax antibodies were from Dako Ltd. (Ely, United Kingdom), anti-PARP antibody was from Alexis Corp. (United Kingdom) Ltd. (Bingham, United Kingdom), and FITC-conjugated annexin V was from Bender MedSystems (Vienna, Austria). Rabbit antisera to NF-κB subunits p50, p65, and RelB were a kind gift of Dr. Nancy Rice (Molecular Basis of Carcinogenesis Laboratory, National Cancer Institute-Frederick Cancer Research and Development Center, Frederick, MD).

NF-κB and AP-1 consensus oligonucleotides were obtained from Promega (Southampton, United Kingdom). All cell culture media and reagents were purchased from Invitrogen (Paisley, United Kingdom).

Cell Lines and Treatments. The human-derived breast carcinoma cell line MDA MB468 and the immortalized non-tumorigenic cell line HBL100[4] were kindly provided by Prof. Rosemary Walker (Department of Pathology, University of Leicester, United Kingdom). Both cell lines are regarded as estrogen receptor-α negative, although they may possess estrogen receptor-β (47). The human-derived prostate carcinoma cell lines DU145 and LNCaP were obtained from American Type Culture Collection (Manassas, VA). The DU145 cell line lacks androgen receptors, whereas the LNCaP cell line is hormone sensitive.

Both breast cell lines were cultured as described previously (48). DU145 cells were cultured in MEM with Earle's Salts containing 2 mM glutamax, supplemented with nonessential amino acids (1×), 1 mM sodium pyruvate, and 10% FCS. The LNCaP cells were cultured in RPMI 1640 supplemented with 2 mM glutamax, 1 mM sodium pyruvate, glucose (1.25 g/500 ml), and 10% FCS. All cell lines were negative when tested for *Mycoplasma* infection. I3C was prepared as a stock solution in DMSO, and cells were treated in such a way that all control and treated cells received equal volumes of DMSO, which did not exceed a final concentration of

[4] Following concerns raised by the American Type Culture Collection that the HBL100 cell line contained a Y chromosome, we had our own stock karyotyped and found it was positive for X only.

0.05%. The purity of the I3C stock in DMSO was verified as approximately 99.9% by HPLC (data not shown). For each experiment, cells were initially seeded in normal growth medium and allowed to adhere for at least 4 h before treatment. The concentrations of I3C used were varied according to the duration of the experiment and the different sensitivities of the cell lines. Lower concentrations of I3C (typically 10–100 μM for the MDA MB468 line and 100–250 μM for the HBL100 cell line) were used in the proliferation and apoptosis studies that were performed over several days and in some Western blots that were performed after 72 h. Higher concentrations of I3C were used in the signaling experiments because these were performed over short time periods (up to 5 h).

Cell Proliferation Studies. Cells were seeded at 5×10^4 onto 6-well plates and cultured in the presence of I3C for times from 72 to 240 h. Approximate IC_{50} values were obtained from a plot of cell number expressed as a percentage of control *versus* I3C concentration. To determine their ability to recover proliferative capacity after treatment, cells (1×10^4 cells on 12-well plates) were cultured in the presence of I3C for 24 h, after which they were either maintained in treated medium or washed and replenished with fresh medium and allowed to recover before harvesting at 168 h. The proliferation rate of cells was calculated as fold increase in cell number after the initial treatment period. For analysis of cell cycle, 5×10^5 cells were seeded onto 9-cm plates and treated with I3C (up to 200 μM) for 48 h. Cells were harvested by trypsinization, fixed overnight in 70% ethanol at 4°C, and then collected by centrifugation, resuspended in PBS containing 0.1 mg/ml RNase and 5 μg/ml propidium iodide, and incubated overnight at 4°C. DNA content was analyzed using a Becton Dickinson FACScan and Cell Quest software. Subsequent data analysis was performed using ModFit LT software (Becton Dickinson United Kingdom Ltd., Cowley, United Kingdom).

Measurement of Phosphatidylserine Externalization. Cells were seeded at 2×10^5, 5×10^5 or 1×10^6 onto 9-cm plates (depending on treatment time) and treated with I3C for times up to 168 h. After treatment, cells obtained by trypsinization were combined with those that had spontaneously detached during the incubation. Phosphatidylserine externalization was determined by annexin V staining. Cells were pelleted and resuspended in 1 ml of annexin buffer [10 mM HEPES (pH 7.4), 150 mM NaCl, 5 mM KCl, 1 mM $MgCl_2$, and 1.8 mM $CaCl_2$]. FITC-conjugated annexin V was added to a final concentration of 100 ng/ml, and cells were incubated for 8 min at room temperature, after which propidium iodide (1.5 μg) was added, and cells were analyzed by flow cytometry using a FACScan flow cytometer and Cell Quest software.

Detection of Total and Phosphorylated PKB, PTEN, Bcl-2, Bcl-xL, and Bax. Cells were seeded at between 1.5 and 3×10^6 onto 9-cm plates, depending on the duration of the experiment, and treated with I3C for 5, 24, 48, or 72 h. In a separate experiment, cells were seeded as described above and cultured for 24 h under normal or serum-depleted (0%) growth conditions or serum-starved for 24 h followed by replenishment of serum (10%) for 4 h. To detect levels of phospho-PKB, PTEN, Bcl-2, Bcl-xL, and Bax, treated cells were lysed in a cell lysis buffer (as detailed in the Akt assay kit) containing 2% (v/v) complete protease inhibitor mixture. Samples were analyzed by SDS-PAGE and immunoblotting, followed by visualization using an enhanced chemiluminescence detection system (Amersham Life Science Ltd., Little Chalfont, United Kingdom). Equal amounts of protein were loaded in each lane. Blots were scanned using a densitometer (Molecular Dynamics, Sunnyvale, CA) and quantified using Image Quant software. In all cases, bands were confirmed as being within the linear range of the film. For determination of total PKB, samples were prepared by washing cells twice in ice-cold PBS and harvesting directly in sample buffer. Samples were then sonicated and boiled for 5 min and analyzed as described above. Loading controls are shown in the figures for blots in which there was a marked change in protein level in response to the treatment. Blots were stripped and reprobed with an anti-tubulin antibody.

Detection of PARP and Its Cleavage Products. Cells were seeded and treated with I3C as described above. Adherent cells were harvested by scraping and combined with those that had detached during the treatment incubation. Cells were then pelleted and subjected to three rounds of freeze thawing before resuspension in 40 μl of sample buffer and sonication. Equal volumes were separated by SDS-PAGE and detected as described above, using an anti-PARP antibody.

Immune Complex Kinase Assay for PKB and IKK. Cells were seeded at $1–2 \times 10^6$ onto 9-cm plates and allowed to adhere. Cultures were treated with I3C for 5 h before harvesting in cell lysis buffer as described above. PKB activity was determined according to the protocol supplied with the Akt kinase assay kit. PKB was immunoprecipitated from 200 μg of cell lysate protein, which gave results within the linear range of the assay. Phosphorylation of the glutathione *S*-transferase-GSK-3 substrate was measured by SDS-PAGE using the phospho-GSK-3α/β antibody, and detection was by chemiluminescence using the Lumiglo detection reagent supplied in the kit. No phosphorylation of the substrate was detected in the absence of PKB.

IKKα was immunoprecipitated from 500 μg of cell lysate protein using an anti-IKKα antibody conjugated to protein A beads and then resuspended in kinase assay buffer as described above. Total IKKα protein levels were detected by SDS-PAGE using the same anti-IKKα antibody. IKKα activity was determined by incubation (30°C, 30 min) with IκBα substrate (1 μg) in the presence of 50 μM ATP (containing 0.074 MBq [γ-^{32}P]ATP). Proteins were separated by SDS-PAGE as described above, and phosphorylated IκBα was detected by PhosphorImager analysis (Molecular Dynamics).

Measurement of Nuclear NF-κB. Cells were seeded and treated as described for the determination of levels of PKB. Nuclear extracts were prepared according to the method of Staal *et al.* (49), and protein content was determined using the Bio-Rad protein assay. Samples were denatured in sample buffer and analyzed by SDS-PAGE as described above, using NF-κB p65, p50, or RelB subunit antibodies.

EMSA for NF-κB DNA Binding. Nuclear extracts were prepared from cells treated with I3C for 5 h, as described above. EMSAs were performed as described previously (50)

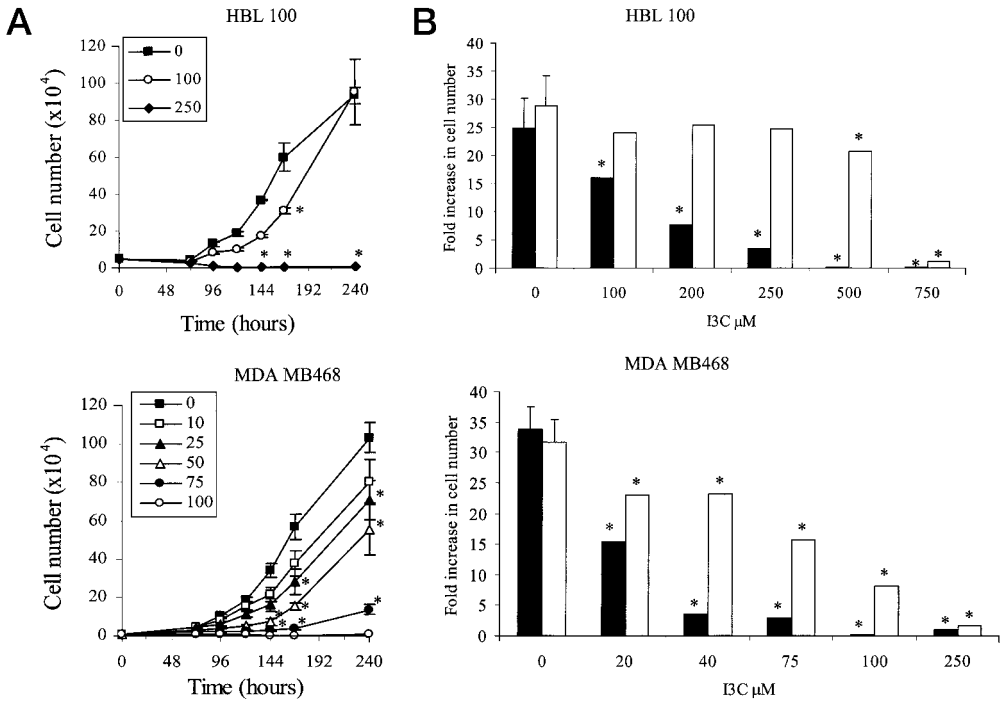

Fig. 1. Effect of I3C on proliferation and recovery of the HBL100 and MDA MB468 cell lines. *A,* growth curves were performed in the presence of increasing concentrations of I3C and counted as detailed in "Materials and Methods." *B,* cells were treated with I3C for 168 h (■) or for 24 h followed by 144 h recovery (□). Data shown are mean cell number ± SE (*A*) or fold increase in cell number ± the SD of the sets (shown on control bars only; *B*). * indicates significant difference from control cell data at that time point ($P < 0.05$), as determined by the ANOVA general linear model followed by Fisher's least significant difference *post hoc* test ($n = 6$).

using a ^{32}P-end labeled NF-κB consensus oligonucleotide (5′-AGT-TGA-GGG-GAC-TTT-CCC-AGG-C-3′) and an excess of either unlabeled NF-κB oligonucleotide or an unrelated AP-1 consensus sequence (5′-CGC-TTG-ATG-AGT-CAG-CCG-GAA-3′).

Statistical Analysis. Statistical significance was assessed using ANOVA balanced or general linear models (51) followed by Fischer's least significant difference *post hoc* test (52).

Results

Inhibition of Cell Growth and Recovery after Treatment with I3C. I3C caused a dose-dependent inhibition of cell proliferation in both cell lines (Fig. 1*A*). However, the MDA MB468 cell line was approximately 4-fold more sensitive to the growth-inhibitory effect of I3C than the HBL100 line, with approximate IC_{50} values (at 168 h) of 30 and 120 μM, respectively. The ability of the two cell lines to recover from I3C treatment also differed markedly. The HBL100 cell line was capable of complete recovery (fold increase in cell number was not significantly different from the control) from 24 h of treatment with concentrations up to 250 μM and almost complete recovery from 500 μM (Fig. 1*B*). In contrast, the MDA MB468 cells only partially recovered from 24 h of treatment with 20 μM I3C and were unable to recover from 24 h of treatment with 250 μM (Fig. 1*B*).

The decrease in cell proliferation caused by I3C may be due to either cytostatic or cytotoxic effects or a combination of both. To determine the nature of the growth inhibition, we determined the effect of I3C on cell cycle progression. No apparent cell cycle phase-specific arrest was observed in either cell line (data not shown), but a clear dose-dependent sub-G_1 peak, indicative of apoptotic cells, was visible in the MDA MB468 cell line only, from 100 μM (Fig. 2*A*).

Induction of Apoptosis by I3C. Using annexin V and propidium iodide staining, we determined the percentage of cells undergoing apoptosis or necrosis by flow cytometry in treated cultures. No increase in the proportion of apoptotic cells was observed for the HBL100 cell line after any dose of I3C. However, as the proportion of live cells decreased over time, a significant dose-dependent increase in the percentage of necrotic cells occurred, from 5% in control cells after 24 h up to 37% in cells treated with 250 μM for 144 h (Fig. 2*B*). Treatment of MDA MB468 cells, on the other hand, resulted in a dose- and time-dependent induction of apoptosis (Fig. 2, *B*–*D*). This was accompanied by a steady increase in the percentage of necrotic cells, which at higher concentrations (500 μM) or longer time points is likely to encompass a proportion of cells undergoing secondary necrosis after apoptosis (Fig. 2). An early increase in apoptosis was detected in the MDA MB468 cells with 500 μM I3C, which reached significance by 8 h (Fig. 2*D*). These results were confirmed by Western analysis of PARP cleavage, in which cleavage products were detected in MDA MB468 cells by 8 h (Fig. 3), whereas in contrast, no such products were readily detected in the HBL100 cell line over the same time

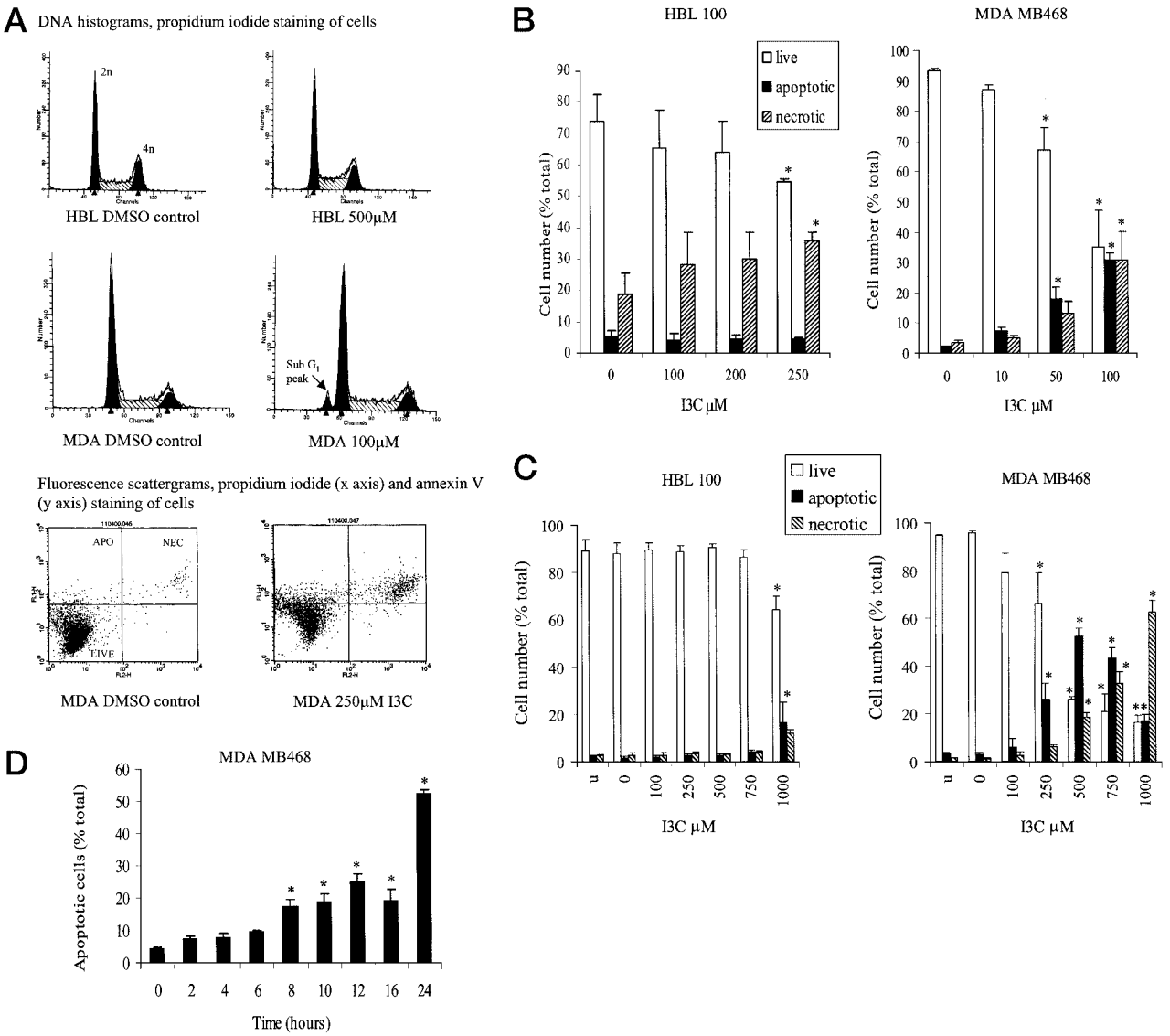

Fig. 2. Effect of I3C on cell cycle progression and induction of apoptosis and necrosis. *A,* sample panels showing flow cytometric analyses of control and treated cells. The *top panels* show DNA content histograms of control and I3C-treated (48 h) HBL100 and MDA MB468 cells determined by propidium iodide staining; the *X* axis shows red fluorescence (propidium iodide), and the *Y* axis represents cell counts. The *bottom panels* show profiles of MDA MB468 cells (24-h treatment) labeled with propidium iodide (shown on the *X* axis) and FITC-conjugated annexin V (*Y* axis); live cells appear in the *bottom left quadrant*, whereas apoptotic (*APO*) and necrotic (*NEC*) cells appear in the *top quadrants* as indicated. The effect of I3C on the proportion of live, apoptotic, or necrotic cells, as determined by annexin V staining in the breast cell lines, is shown after 144 h in *B* and 24 h in *C*. A time course (0–24 h) for the induction of apoptosis by I3C (500 μM) in the MDA MB468 cell line is shown in *D*. Results shown are mean $\pm$ SE ($n = 3$). $*$ indicates significant difference from the control (DMSO-treated) group ($P < 0.05$) as determined by the ANOVA balanced model followed by Fisher's least significant difference *post hoc* test.

course. To ensure that even a small amount of cleaved product was detected if present in the HBL100 cell line, a high amount of protein was loaded onto the gel, and a long film exposure time was used. The data were interpreted with respect to cleavage or noncleavage of the protein and not to any change in the relative amount of full-length protein.

Effect of I3C on PKB Levels and Phosphorylation. We next investigated whether the induction of apoptosis by I3C in the MDA MB468 cell line could be due to inhibition of signaling via the prosurvival protein kinase PKB. The tumor cells were found to have approximately 3-fold higher basal levels of phospho-PKB than the HBL100 cell line, although the latter had higher total PKB protein levels (Fig. 4).

Whereas there was no intentional stimulation of PKB phosphorylation, it should be noted that in the MDA MB468 cell line only, the level of phosphorylated PKB (both sites) was increased in the DMSO-treated control compared with untreated cells ($P < 0.05$).

In these and subsequent experiments, we used higher concentrations of I3C than in the longer-term apoptosis and growth studies to elicit a fast response and investigate the early events that precede induction of apoptosis in response

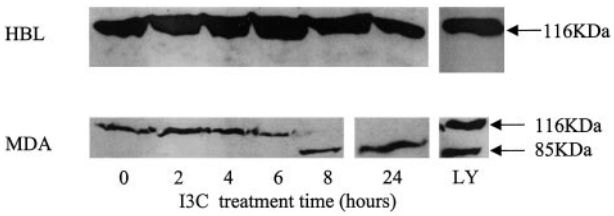

Fig. 3. Cleavage of PARP in HBL100 and MDA MB468 cells in response to I3C (500 μM; 0–24 h) or LY294002 (50 μM; 24 h). The blots shown are representative of two or more independent experiments. In these experiments, to ensure detection of potentially very low levels of cleaved PARP (if present) in the HBL100 cell line, a high amount of protein was loaded onto the gel, and a long film exposure was used.

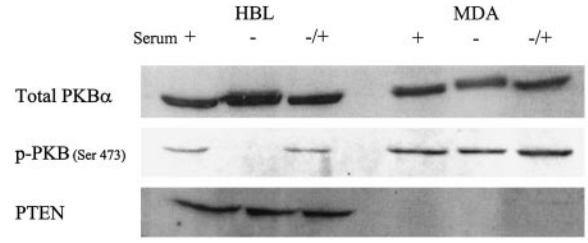

Fig. 4. Representative blots showing comparative basal levels of total PKBα protein, phospho-PKB (Ser 473), and PTEN in the HBL100 and MDA MB468 cell lines. *Lane 1* (+), protein levels from cells cultured under normal growth conditions (10% FCS); *Lane 2* (−), protein levels from cells after 24 h of serum starvation; *Lane 3* (−/+), protein levels 4 h after replenishment of serum (10%) to starved cells.

to the agent. Concentrations of up to 1 mM were used in some instances to confirm any apparent absence of treatment-related effects on components of a pathway. Treatment with I3C for 5 h resulted in a dose-dependent decrease in basal levels of phosphorylated PKB in the MDA MB468 cell line compared with the DMSO control but had no effect in the HBL100 cell line (Fig. 5*A*). This was detected using antibodies specific to either the Ser-473 or Thr-308 phosphorylation sites. In the HBL100 cell line, whereas there was clearly no decrease in phosphorylation at the Ser-473 site, phospho-PKB was not detectable using the antibody to the Thr-308 phosphorylation site. Thus, the Ser 473 antibody was used in subsequent experiments. The decrease in phospho-PKB was also time dependent, and treatment with 500 μM I3C resulted in a gradual decrease in phospho-Akt (Ser 473) levels to approximately 50% after 5 h (data not shown). I3C (0–1000 μM, 5 h) did not decrease PKB protein levels in either cell line, indicating that the decrease in phospho-PKB observed in the MDA MB468 cells under the same conditions was due to a decrease in the phosphorylation status of the protein (Fig. 5, *A* and *B*). Treatment with the phosphatase 2A inhibitor okadaic acid resulted in a dose-dependent increase in phospho-PKB levels in both breast cell lines, but pretreatment with okadaic acid (10, 25, or 50 nM, 2 h before I3C treatment for 5 h) did not protect against the I3C-induced decrease in phosphorylated PKB in the MDA MB468 cell line (data not shown). It is noteworthy that treatment with okadaic acid caused severe toxicity to the MDA MB468 cells at concentrations above 25 nM, whereas the HBL100 cells tolerated concentrations up to 100 nM.

Effect of I3C on PKB Activity. PKB activity, as determined by *in vitro* kinase assay, was also found to be decreased in a dose-dependent manner after I3C treatment (5 h) in the MDA MB468 cell line, but not in the HBL100 line (Fig. 5, *C* and *D*, data shown for MDA MB468 only), corresponding to the effect of I3C on the levels of phosphorylated PKB in each cell line. I3C (up to 750 μM) had no effect on the kinase activity when added directly to the assay, although at the higher concentration (1000 μM) there was slight evidence for direct inhibition of PKB activity (Fig. 5*C*).

Effect of I3C on the PTEN Tumor Suppressor. The tumor suppressor PTEN has been shown to dephosphorylate PI3K-generated phosphatidylinositol 3,4,5-trisphosphate molecules (45), which are required for the activation of PKB (reviewed in Refs. 33 and 44). We therefore examined the levels of PTEN in the cell lines and found that they were inversely correlated with phospho-PKB, with the HBL100 cell line expressing substantial levels, whereas in the MDA MB468 line, PTEN was not generally detected (Fig. 4). I3C (0–1000 μM, 24 h) had no significant effect on PTEN levels in either cell line (data not shown).

Inhibition of PKB and Induction of Apoptosis by LY294002. PKB is activated via a PI3K-generated phospholipid-dependent mechanism, leading to the phosphorylation of PKB by at least one 3-phosphoinositide-dependent kinase (reviewed in Ref. 33). To determine whether inhibition of PKB was sufficient for the induction of apoptosis in the MDA MB468 line, we investigated the effect of the PI3K inhibitor LY294002 on PKB phosphorylation and induction of apoptosis. In contrast to I3C, LY294002 (50 μM) inhibited PKB phosphorylation in both cell lines (Fig. 6). In the MDA MB468 cell line, LY294002 treatment clearly resulted in induction of apoptosis after 24 h, as detected by PARP cleavage, whereas very little evidence of apoptosis was observed in the HBL100 cell line (Fig. 3).

Effect of I3C on the Prostate Cell Lines DU145 and LNCaP. To investigate whether the proapoptotic and PKB-inhibitory effect of I3C was specific to cell lines with undetectable or very low levels of PTEN, we investigated the effect of I3C on LNCaP and DU145 prostate cell lines, which express different levels of phospho-PKB and PTEN (Fig. 7*A*). Densitometric analysis of Western blots showed the DU145 cells to have the highest levels of PTEN (twice that of HBL100 cells and approximately 6-fold higher than LNCaP cells) with barely detectable levels of phospho-PKB, whereas the LNCaP cells, like the MDA MB468 cells, expressed much higher levels of phospho-PKB with low PTEN (Fig. 7*A*). Although less marked than in the breast cells, I3C inhibited growth of the high phospho-PKB-expressing LNCaP cell line to a greater extent than the DU145 cell line, with approximate IC_{50} values of 22 and 48 μM (data not shown).

I3C (5 h of treatment) caused a dose-dependent decrease in phospho-PKB levels in the LNCaP cell line, with no obvious effect in the DU145 line (Fig. 7*B*). LY29004 completely abolished phospho-PKB in both cell lines. In agreement with results obtained with the breast cells, the high phospho-PKB/low PTEN-expressing cell line LNCaP, but not DU145

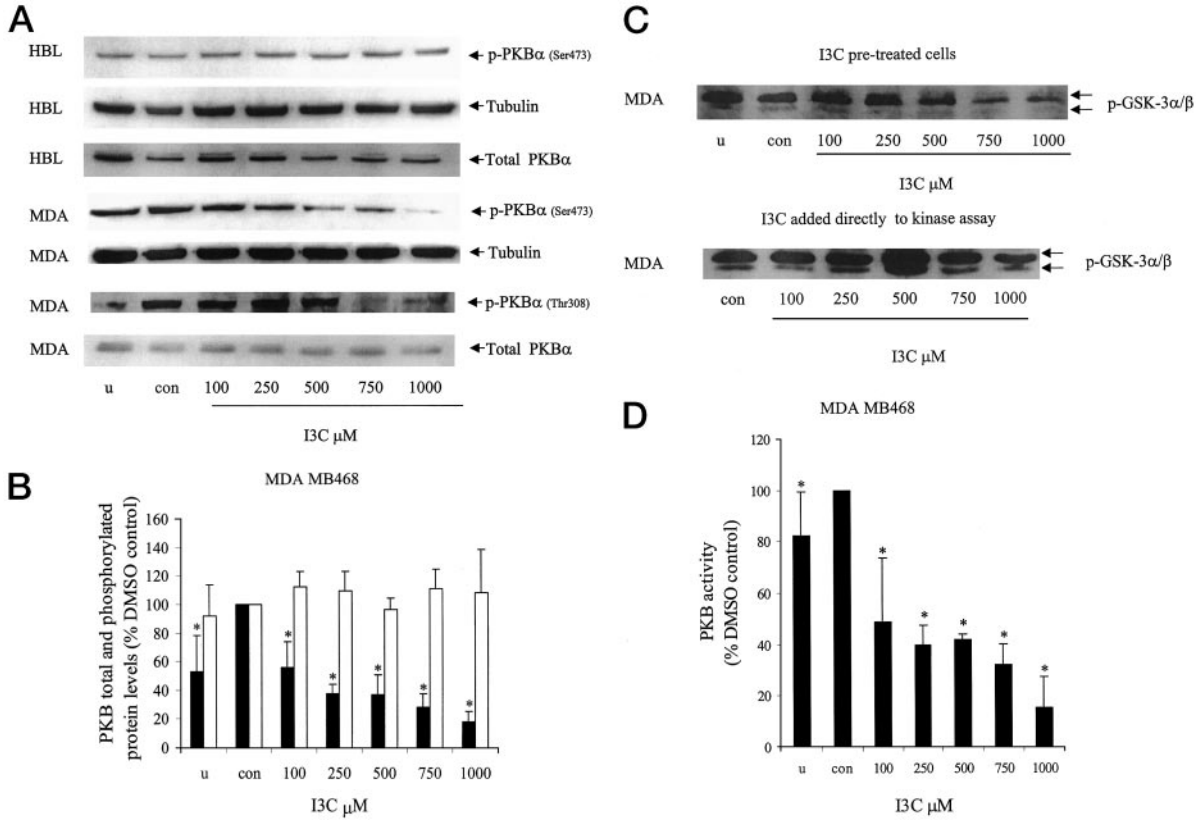

Fig. 5. Effect of I3C on PKB levels (*A* and *B*) and activity (*C* and *D*). *A,* representative Western blots for HBL100 and MDA MB468 showing the effect of increasing concentrations of I3C (5-h treatment) on levels of phospho-PKB (Ser 473 and Thr 308) and total PKB [blot shown is with an antibody to total (non-phospho-specific) PKBα, which gave results in agreement with an antibody that detects all three isoforms (data shown in *B*)]. Tubulin loading controls are shown for HBL100 and MDA MB468 phospho-PKB (Ser 473) blots. *B,* effect of I3C on total (□) and phospho-PKB levels (■) in the MDA MB468 cell line. Data shown are mean ± SE ($n = 3$) of values obtained by densitometric analysis of Western blots and are expressed as a percentage of the DMSO control. *C,* representative Western blots showing PKB activity determined by phosphorylation of a glutathione *S*-transferase-GSK-3α/β substrate in an *in vitro* kinase assay. PKB activity was assayed in extracts from MDA MB468 cells treated with I3C as described above (*top panel*) and in extracts from untreated MDA MB468 cells when I3C was added directly to the kinase assay (*bottom panel*). *D,* effect of I3C on PKB activity. Data shown are mean ± SE ($n = 3$) of values obtained by densitometry as described in *B*. The blots shown in *A* and *C* are representative of three independent experiments. It should be noted that the exposure times of the blots shown in *A* were not identical. *Bars* in *B* and *D* marked * are significantly different ($P < 0.05$) from the control levels, as determined by the ANOVA balanced model followed by Fisher's least significant difference *post hoc* test. *Lanes* marked *u* and *con* indicate no treatment and the DMSO control, respectively.

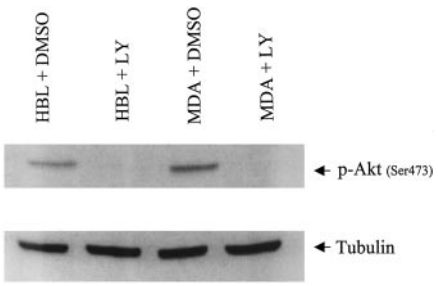

Fig. 6. Effect of LY294002 (5 h, 50 μM) on levels of phospho-PKB (Ser 473) in HBL100 and MDA MB468 cell lines. The blot shown is representative of results obtained on more than three occasions. The *bottom panel* shows a tubulin loading control for the phospho-PKB blot.

cells, underwent significant apoptosis after treatment with LY294002 for 24 h (Fig. 7*C*). Furthermore, the LNCaP cell line was also more sensitive to induction of apoptosis by I3C (24 h), showing a consistently greater fold increase in the proportion of apoptotic cells relative to control with each treatment (Fig. 7*C*). The LNCaP cells undergo a higher basal rate of apoptosis (approximately 9% in control cells compared with 6% in control DU145 cells), suggesting that they may be predisposed to cell death via this mechanism. The increase in necrosis that occurred alongside the increase in apoptosis in the LNCaP cells after I3C treatment may represent secondary necrosis of previously apoptotic cells.

Effect of I3C on Bcl-2, Bcl-xL, and Bax. In a recent study, Rahman *et al.* (23) showed an increase in the ratio of Bax to Bcl-2 in T47D cells in response to I3C, thus favoring apoptosis. PKB has been implicated in the transcriptional regulation of Bcl-2 (41), and therefore a decrease in Bcl-2 seemed a likely candidate for mediating the apoptotic effect of PKB inhibition by I3C. We found no evidence of a decrease in Bcl-2 or an increase in Bax after 5 or 24 h of treatment with I3C (Fig. 8*A*, 5 h data). However, at 48 and 72 h, levels of Bcl-2 were decreased in both cell lines, although the data did not show a clear dose response (Fig. 8*B*, 48 h data). Levels

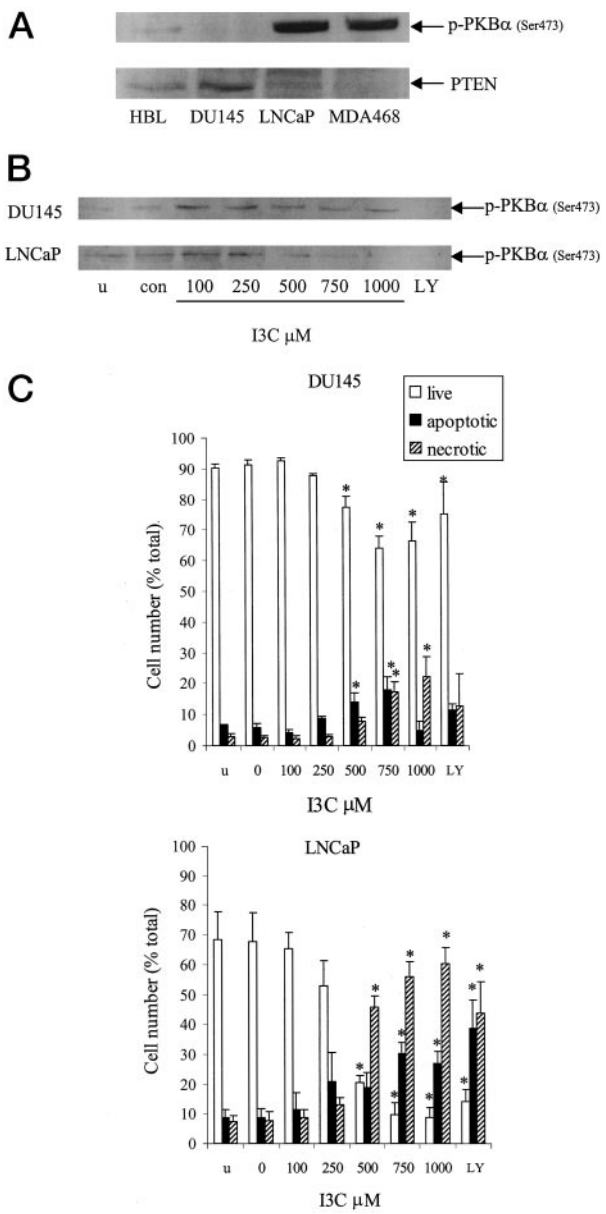

Fig. 7. Effect of I3C on PKB phosphorylation and induction of apoptosis in the prostate cell lines DU145 and LNCaP. *A,* representative blots of phospho-PKB and PTEN levels in the two prostate cell lines, together with the MDA MB468 and HBL100 cell lines. The effect of I3C (5-h treatment) on phospho-PKB in the prostate cells is shown in *B*. Induction of apoptosis and necrosis in response to I3C and LY294002 (24-h treatment) is shown in *C*. Data are mean ± SE ($n = 3$); * indicates significant difference from the control (DMSO-treated) group ($P < 0.05$) as determined by the ANOVA balanced model followed by Fisher's least significant difference *post hoc* test.

of Bcl-xL were decreased in the MDA MB468 cells at ≥375 μM and in the HBL100 line at 500 μM after only 24 h (Fig. 8*C*). Because the effects on these apoptotic regulatory proteins were not observed until the 24 or 48 h time points, occurred in both cell lines, and were not always clear cut, it is unlikely that they constitute a major mechanism by which I3C initiates apoptosis in the MDA MB468 cell line, but they could well contribute to its progression.

Effect of I3C on IKK Activity and Nuclear Levels of NF-κB. NF-κB is one of the prosurvival factors that lie downstream of PKB signaling. PKB has been shown to regulate NF-κB via activation of the IKK complex, resulting in enhanced NF-κB DNA binding and transactivational activity (53, 54). Treatment with I3C (5 h) had no effect on IKK activity as measured by *in vitro* kinase assay using IκBα as a substrate (Fig. 9*A*) or on total IKK protein levels (data not shown). In support of this, levels of nuclear NF-κB (p65) remained unchanged after a 5-h treatment of either cell line (Fig. 9*B*). Interestingly, nuclear NF-κB p65 and p50 levels were not depleted after serum starvation in either cell line, whereas RelB was reduced in both cell lines (Fig. 9*C*), suggesting that the presence of transcriptionally active NF-κB in the nucleus is constitutive in these cell lines.

Effect of I3C on NF-κB DNA Binding. We next used EMSA to investigate the effect of I3C on binding of proteins to the NF-κB DNA recognition site. Binding of nuclear extracts from either cell line to a NF-κB DNA consensus sequence resulted in formation of a specific pattern of binding consisting of a slower-migrating doublet and two faster-migrating bands. The specificity of all of the bands was confirmed by competition assays using a 200× molar excess of unlabeled NF-κB consensus oligonucleotide or an unrelated sequence.

Using nuclear extracts prepared from MDA MB468 cells treated with I3C for 5 h, we found a decrease in specific protein interaction with the NF-κB DNA sequence (Fig. 9*D*). In contrast, nuclear extracts from the HBL100 cell line showed an apparent increase in protein binding (Fig. 9*D*). In both cases, this suggests that I3C can cause alteration in DNA binding of NF-κB protein family members independently of changes in nuclear NF-κB levels and IKK activity. In separate supershift experiments, we confirmed the presence of both p65 and p50 in the DNA-binding protein complex (Fig. 9*D*).

Discussion

Results presented in this study show clearly that the antiproliferative effect of the chemopreventive agent I3C is cell type specific even between cells from one tissue but that modulation of cell signaling pathways and induction of apoptosis can contribute to its mechanism of action in breast and prostate tumor cells. We showed that the MDA MB468 breast tumor cell line underwent apoptosis after treatment with I3C in a dose- and time-dependent manner, as assessed by measurement of phosphatidylserine externalization and confirmed by PARP cleavage. Apoptosis was detected by 72 h in MDA MB468 cells treated with 10 μM I3C and as early as 6 h in MDA MB468 cells treated with 500 μM I3C. In contrast, the nontumorigenic HBL100 cell line was resistant to induction of apoptosis by concentrations of I3C up to 1 mM but did show an increase in the percentage of necrotic cells after 96 h of treatment with 200 μM I3C and above. It is likely that this differential induction of apoptosis accounts for the approximate 4-fold difference in sensitivity in terms of growth inhibition between the two cell lines. This would also explain the inability of the MDA MB468 cells to recover from treatment once they have become committed

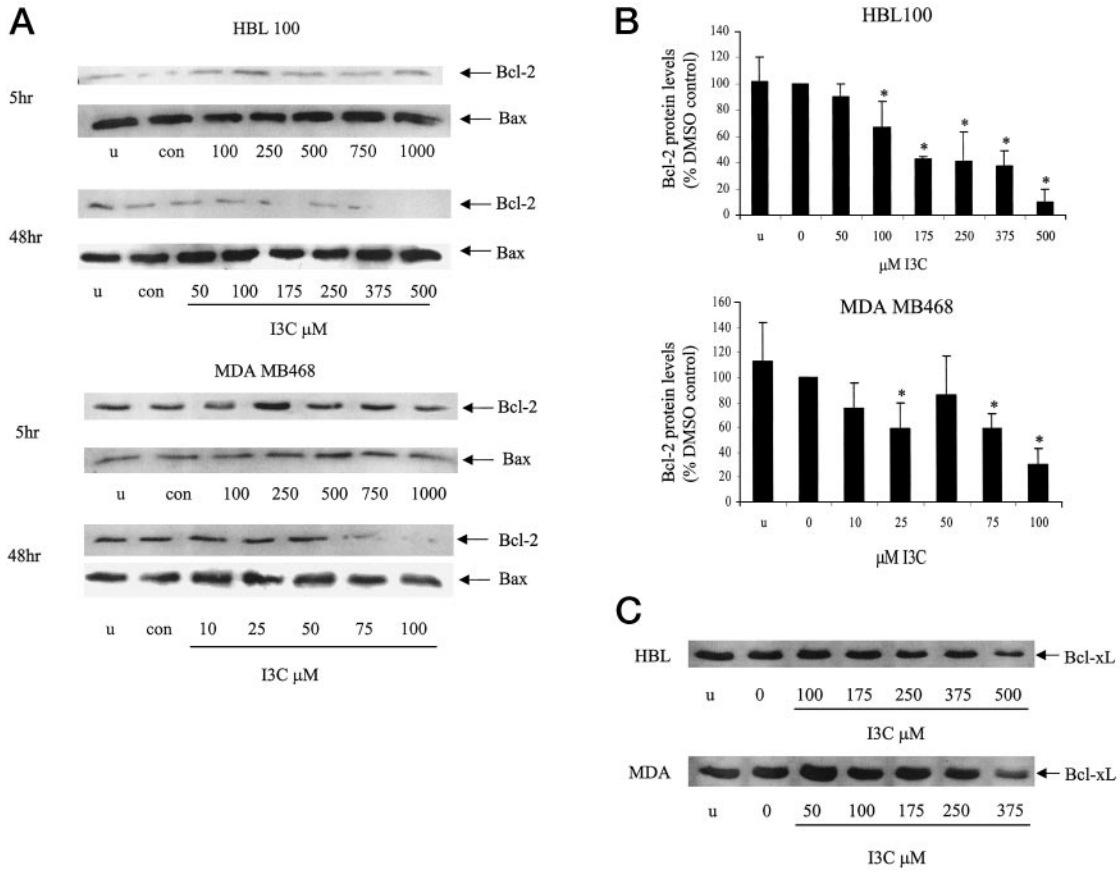

Fig. 8. Effect of I3C on levels of Bcl-2, Bax, and Bcl-xL. *A,* representative blots of Bcl-2 and Bax after 5 or 48 h of treatment with I3C. Blots are representative of at least three experiments. Densitometric analysis of data from the 48 h time point is shown in *B*. Data shown are the mean ± SD expressed as a percentage of the DMSO-treated control. * indicates significant difference from the DMSO-treated control. *C,* effect of I3C on Bcl-xL protein levels after 24 h (blot is representative of at least three separate experiments).

to the apoptotic process, in contrast to the HBL100 cell line, which undergoes necrosis only and recovers readily once I3C is removed from the culture medium. These data indicate a fundamental difference in the mechanism by which I3C exerts growth-inhibitory effects in these two cell lines.

To investigate the mechanistic effects of I3C at early time points and also, in some cases, to rule out any potential mechanistic role of a pathway, particularly in the more resistant HBL100 cell line, we used concentrations of the agent above 500 μM. It should be noted that whereas these experiments provided useful mechanistic data, concentrations of I3C above 500 μM are unlikely to have any relevance to a physiological situation.

To investigate the differential response of the two cell lines, components of the PKB pathway were examined. Despite the higher levels of total PKB protein found in the HBL100 cell line, the MDA MB468 cell line had higher levels of the phosphorylated form. Whereas PTEN, which blocks activation of PKB by dephosphorylation of PI3K signaling intermediates, was expressed in the HBL100 cell line (lower phospho-PKB expression), we did not detect it in the MDA MB468 cell line (high phospho-PKB). These data are in agreement with a report by Lu *et al.* (55), in which it was shown that loss of function of PTEN in breast cancer cell lines, including MDA MB468, resulted in increased basal phosphorylation of multiple components of the PI3K signaling pathway. We conclude therefore that the presence of PTEN in the HBL100 cell line accounts for its lower level of phospho-PKB in comparison with the MDA MB468 cell line. Together, these observations would seem to signify a heightened importance of signaling through the PKB pathway in the MDA MB468 cell line relative to the HBL100 cell line.

PKB has been well documented as a prosurvival factor (26, 32, 33, 37, 39, 41–43) and has also been implicated in oncogenesis (39, 44, 56, 57). I3C (5-h treatment) decreased basal levels of phosphorylated PKB and PKB activity in the MDA MB468 cell line, but not in the HBL100 cell line. I3C did not inhibit PKB activity when added directly to an *in vitro* kinase assay at concentrations up to 750 μM, indicating that it was not acting as a direct enzyme inhibitor. Over an 8-h treatment period, no decrease in total PKB protein level was observed, strongly suggesting that I3C acts on signaling pathways upstream of PKB. Because the effect was not prevented by pretreatment with the phosphatase 2A inhibitor okadaic acid, it seems most likely that I3C acts by preventing phosphorylation of the protein rather than by promoting its dephosphorylation. Recent results reported by Meng *et al.* (58) showed induction of PTEN by I3C in the T47D breast cell

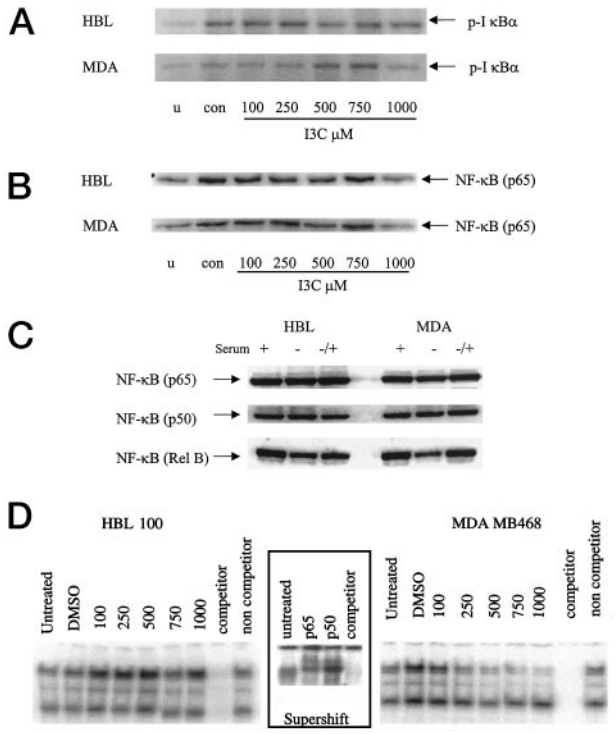

Fig. 9. Effect of I3C (0–1000 μM; 5 h) on IKK activity as determined by phosphorylation of IκBα in an *in vitro* kinase assay (*A*) and on nuclear NF-κB (p65) levels (*B*). *C* shows nuclear levels of NF-κB (p65, p50, and RelB) in cells cultured under normal growth conditions (+), after 24 h of serum starvation (−), and 4 h after replenishment of serum-starved cells with 10% FCS (−/+). *D* shows the effect of I3C on NF-κB DNA binding as measured by EMSA in HBL100 and MDA MB468 cell lines. The blots shown are representative of three independent experiments. Supershift of p65 and p50 in control HBL100 cells is shown in the *boxed area* of *D*.

line. However, in our study, I3C did not appear to stimulate PTEN levels in either MDA MB468 or HBL100 cell lines.

Inhibition of PKB phosphorylation in both breast cell lines by the specific PI3K inhibitor LY294002 still only induced apoptosis significantly in the MDA MB468 cell line. This observation led us to two conclusions: (*a*) first, because inhibition of PKB by LY294002 induced apoptosis in the MDA MB468 cell line, it is likely that such inhibition contributes to the I3C-induced apoptosis observed in this cell line; and (*b*) second, the HBL100 cell line was resistant to induction of apoptosis by LY294002, despite a decrease in phospho-PKB levels, indicating that other survival signaling pathways predominate in this cell line. We also have preliminary data (not shown here) for two additional human breast tumor-derived cell lines, T47D and MCF7, both of which are positive for PTEN. Levels of PTEN were similar in MCF7 and HBL100 cell lines and higher in the T47D line. Levels of phospho-Akt in the T47D cell line were similar to those in the HBL100 cell line, and lower than those in the MCF7 cell line. I3C inhibited the growth of these cell lines with an approximate IC_{50} of 60 μM and, as in the HBL100 cell line, did not show inhibition of phospho-PKB levels after a 5-h treatment.

We propose that the sensitivity of the MDA MB468 cell line to I3C stems at least in part from the relative importance of signaling through the PKB pathway in this cell line compared with that in the PTEN-positive HBL100 cell line. To strengthen the idea that the cell-specific effects of I3C in the breast cell lines were related to their relative phospho-PKB levels and PTEN status, we determined the effect of the agent in prostate cells of known PTEN status. In agreement with our hypothesis, I3C decreased phospho-PKB levels and induced apoptosis in the LNCaP cell line, which expresses very low levels of PTEN, but not in the DU145 cell line, which expresses much higher levels of PTEN. Our data are also consistent with a report by Hsu *et al.* (59), in which the cyclooxygenase-2 inhibitor celecoxib was shown to induce apoptosis in the prostate carcinoma cell lines LNCaP and PC-3 by a mechanism involving PKB (59). As with I3C, celecoxib had no effect on Bcl2 levels at short time points, and the inhibition of PKB phosphorylation was not prevented by okadaic acid. Hsu *et al.* (59) also observed no inhibition of PI3K activity in response to celecoxib in prostate cell lines. Our finding that the PI3K inhibitor LY294002 decreased phosphorylation of PKB in all four cell lines in contrast to the cell line-specific effect of I3C indicated to us that the mechanism by which I3C acts upstream of PKB does not consist of a straightforward inhibition of PI3K activity (again showing similarity to celecoxib). Extensive investigations are currently under way in our laboratory to elucidate the possible involvement of differential expression of upstream targets including the epidermal growth factor receptor in the mechanism of action of I3C.

A possible candidate for mediating the effects of I3C-induced inhibition of PKB signaling is the prosurvival transcription factor NF-κB. PKB can regulate NF-κB via activation of IKK, resulting in increased phosphorylation of IκB and consequent release of NF-κB from the inhibitory complex (53, 54). Despite inhibition of PKB, we found no decrease in IKK activity in either cell line in response to I3C treatment. In support of this, nuclear levels of NF-κB (p65) also remained unchanged. However using EMSA, we found that binding to an NF-κB consensus oligonucleotide was decreased using nuclear protein extracts from I3C-treated MDA MB468 cells, but not in those from the HBL100 cell line. From these results, we concluded that I3C alters DNA binding of NF-κB protein family members, including p65 and p50, by a mechanism that does not involve inhibition of IKK activity. The constitutive expression of NF-κB in the nucleus of HBL100 and MDA MB468 cells points to the possibility that in these cell lines translocation of the protein to the nucleus may not be the major limiting step in NF-κB-induced transactivation. The cell line specificity of the inhibition of DNA binding by I3C corresponded with that observed for inhibition of PKB, suggesting that the decrease in NF-κB DNA binding may occur as a consequence of inhibition of PKB activity or of a common upstream regulatory step. Recently, Heiss *et al.* (60) showed that sulforaphane, an aliphatic isothiocyanate also found in cruciferous vegetables, inhibited NF-κB DNA binding in macrophages. The mechanism by which sulforaphane exerted this effect was independent of IκB degradation or translocation of NF-κB to the nucleus, and a redox-dependent mechanism was proposed (60). There are other examples in the literature in which modulation of nuclear NF-κB DNA binding has been found to occur independently of effects on IKK or nuclear translocation (61–64). The mechanism by which I3C affects NF-κB DNA binding in the MDA MB468 cell line remains to be confirmed.

This is the first study to show selectivity in the response to I3C between normal- and tumor-derived human cell lines and between cell lines of differing phospho-PKB and PTEN status. The MDA MB468 tumor cell line was 4-fold more sensitive to the growth-inhibitory effects of I3C and, in contrast to the immortalized HBL100 line, underwent apoptosis in response to 10 μM I3C. We propose that inhibition of the PKB signaling pathway contributed to the induction of apoptosis observed in response to I3C in this cell line. Our data also suggest that this effect may be at least partly mediated downstream of PKB by inhibition of NF-κB DNA binding activity. The MDA MB468 cell line is regarded as negative for estrogen receptor-α and with its high level of epidermal growth factor receptor expression, it is therefore representative of an aggressive breast tumor phenotype that typically affects younger women. This finding therefore has promising implications for the use of I3C as a treatment in women with aggressive, estrogen-insensitive breast cancer and as a preventive agent in women at high risk.

Acknowledgments

We thank Dr. D. Alessi (School of Life Sciences Research Biocentre, University of Dundee) and Dr. M. MacFarlane (Medical Research Council Toxicology Unit, University of Leicester) for most helpful discussion and Dr. M. Williams and M. Anderton (Department of Oncology, University of Leicester) for analysis of the I3C stock. We are grateful to Ruth Barber (Department of Genetics, University of Leicester) for the chromosomal analysis of the HBL100 cell line.

References

1. Manson, M. M., Hudson, E. A., Ball, H. W. L., Barrett, M. C., Clark, H. L., Judah, D. J., Verschoyle, R. D., and Neal, G. E. Chemoprevention of aflatoxin B_1-induced carcinogenesis by indole-3-carbinol in rat liver: predicting the outcome using early biomarkers. Carcinogenesis (Lond.), *19:* 1829–1836, 1998.

2. Tanaka, T., Kojima, T., Morishita, Y., and Mori, H. Inhibitory effects of the natural products indole-3-carbinol and sinigrin during initiation and promotion phases of 4-nitroquinoline 1-oxide-induced rat tongue carcinogenesis. Jpn. J. Cancer Res., *83:* 835–842, 1992.

3. Grubbs, C. J., Steele, V. E., Casebolt, T., Juliana, M. M., Eto, I., Whitaker, L. M., Dragnev, K. H., Kelloff, G. J., and Lubet, R. L. Chemoprevention of chemically-induced mammary carcinogenesis by indole-3-carbinol. Anticancer Res., *15:* 709–716, 1995.

4. Srivastava, B., and Shukla, Y. Antitumour promoting activity of indole-3-carbinol in mouse skin carcinogenesis. Cancer Lett., *134:* 91–95, 1998.

5. Rosen, C. A., Woodson, G. E., Thompson, J. W., Hengesteg, A. P., and Bradlow, H. L. Preliminary results of the use of indole-3-carbinol for recurrent respiratory papillomatosis. Otolaryngol. Head Neck Surg., *118:* 810–815, 1998.

6. Bell, M. C., Crowley-Nowick, P., Bradlow, H. L., Sepkovic, D. W., Schmidt-Grimminger, D., Howell, P., Mayeaux, E. J., Tucker, T. E., Turbat-Herrera, E. A., and Mathis, J. M. Placebo-controlled trial of indole-3-carbinol in the treatment of CIN. Gynecol. Oncol., *78:* 123–129, 2000.

7. Wong, G. Y. C., Bradlow, L., Sepkovic, D., Mehl, S., Mailman, J., and Osborne, M. P. Dose-ranging study of indole-3-carbinol for breast cancer prevention. J. Cell. Biochem. Suppl., *28–29:* 111–116, 1997.

8. Cover, C. M., Hsieh, S. J., Cram, E. J., Hong, C., Riby, J. E., Bjeldanes, L. F., and Firestone, G. L. Indole-3-carbinol and tamoxifen cooperate to arrest the cell cycle of MCF-7 human breast cancer cells. Cancer Res., *59:* 1244–1251, 1999.

9. Shertzer, H. G., Berger, M. L., and Tabor, M. W. Intervention in free-radical mediated hepatotoxicity and lipid-peroxidation by indole-3-carbinol. Biochem. Pharmacol., *37:* 333–338, 1988.

10. Manson, M. M., Ball, H. W. L., Barrett, M. C., Clark, H. L., Judah, D. J., Williamson, G., and Neal, G. E. Mechanism of action of dietary chemopreventive agents in rat liver: induction of Phase I and II drug metabolising enzymes and aflatoxin B_1 metabolism. Carcinogenesis (Lond.), *18:* 1729–1733, 1997.

11. Goeger, D. E., Shelton, D. W., Hendricks, J. D., and Bailey, G. S. Mechanisms of anti-carcinogenesis by indole-3-carbinol: effect on the distribution and metabolism of aflatoxin B_1 in rainbow trout. Carcinogenesis (Lond.), *7:* 2025–2031, 1986.

12. Dashwood, R. H., Arbogast, D. N., Fong, A. T., Hendricks, J. D., and Bailey, G. S. Mechanisms of anti-carcinogenesis by indole-3-carbinol: detailed *in vivo* DNA binding dose-response studies after dietary administration with aflatoxin B_1. Carcinogenesis (Lond.), *9:* 427–432, 1988.

13. Dashwood, R. H., Arbogast, D. N., Fong, A. T., Pereira, C., Hendricks, J. D., and Bailey, G. S. Quantitative inter-relationships between aflatoxin B_1 carcinogen dose, indole-3-carbinol anti-carcinogen dose, target organ DNA adduction and final tumour response. Carcinogenesis (Lond.), *10:* 175–181, 1989.

14. Stresser, D. M., Bailey, G. S., and Williams, D. E. Indole-3-carbinol and β-naphthoflavone induction of aflatoxin B_1 metabolism and cytochromes P450 associated with bioactivation and detoxification of aflatoxin B_1 in the rat. Drug Metab. Dispos., *22:* 383–391, 1994.

15. Stresser, M., Williams, D. E., McLellan, L. I., Harris, T. M., and Bailey, G. S. Indole-3-carbinol induces a rat-liver glutathione transferase subunit (Yc2) with high activity toward aflatoxin B_1 exo-epoxide. Association with reduced levels of hepatic aflatoxin DNA adducts *in vivo*. Drug Metab. Dispos., *22:* 392–399, 1994.

16. Hayes, J. D., Judah, D. J., McLellan, L. I., and Neal, G. E. Contribution of glutathione *S*-transferases to the mechanisms of resistance to aflatoxin B_1. Pharmacol. Ther., *50:* 443–472, 1991.

17. Judah, D. J., Hayes, J. D., Yang, J-C., Lian, L-Y., Roberts, G. C. K., Farmer, P. B., Lamb, J. H., and Neal, G. E. A novel aldehyde reductase with activity towards a metabolite of aflatoxin B_1, is expressed in rat liver during carcinogenesis and following the administration of an antioxidant. Biochem. J., *292:* 13–18, 1993.

18. Manson, M. M., Gescher, A., Hudson, E. A., Plummer, S. M., Squires, M. S., and Prigent, S. A. Blocking and suppressing mechanisms of chemoprevention by dietary constituents. Toxicol. Lett., *112–113:* 499–505, 2000.

19. Manson, M. M., Holloway, K. A., Howells, L. M., Hudson, E. A., Plummer, S. M., Squires, M. S., and Prigent, S. A. Modulation of signal-transduction pathways by chemopreventive agents. Biochem. Soc. Trans., *28:* 7–12, 2000.

20. Sharma, S., Stutzman, J. D., Kelloff, G. J., and Steele, V. E. Screening of potential chemopreventive agents using biochemical markers of carcinogenesis. Cancer Res., *54:* 5848–5855, 1994.

21. Cover, C. M., Hsieh, S. J., Tran, S. H., Hallden, G., Kim, G. S., Bjeldanes, L. F., and Firestone, G. L. Indole-3-carbinol inhibits the expression of cyclin-dependent kinase-6 and induces a G_1 cell cycle arrest of human breast cancer cells independent of estrogen receptor signalling. J. Biol. Chem., *273:* 3838–3847, 1998.

22. Telang, N. T., Katdare, M., Bradlow, H. L., Osborne, M. P., and Fishman, J. Inhibition of proliferation and modulation of estradiol metabolism: novel mechanisms for breast cancer prevention by the phytochemical indole-3-carbinol. Proc. Soc. Exp. Biol. Med., *216:* 246–252, 1997.

23. Rahman, K. M. W., Aranha, O., Glazyrin, A., Chinni, S. R., and Sarkar, F. H. Translocation of Bax to mitochondria induces apoptotic cell death in indole-3-carbinol (I3C) treated breast cancer cells. Oncogene, *19:* 5764–5771, 2000.

24. Ge, X., Fares, F. A., and Yannai, S. Induction of apoptosis in MCF-7 cells by indole-3-carbinol is independent of p53 and Bax. Anticancer Res., *19:* 3199–3204, 1999.

25. Ge, X., Yannai, S., Rennert, G., Gruener, N., and Fares, F. A. 3,3′-Diindolylmethane induces apoptosis in human cancer cells. Biochem. Biophys. Res. Commun., *228:* 153–158, 1996.

26. Cross, T. G., Scheel-Toeller, D., Henriquez, N. V., Deacon, E., Salmon, M., and Lord, J. M. Serine/threonine protein kinases and apoptosis. Exp. Cell Res., *256:* 34–41, 2000.

27. Chen, Y-R., Zhou, G., and Tan, T-H. c-Jun N-terminal kinase mediates apoptotic signaling induced by *N*-(4-hydroxyphenyl)retinamide. Mol. Pharmacol., *56:* 1271–1279, 1999.

28. Du, J., Suzuki, H., Nagase, F., Akhand, A. A., Yokoyama, T., Miyata, T., Kurokawa, K., and Nakashima, I. Methylglyoxal induces apoptosis in Jurkat leukemia T cells by activating c-Jun N-terminal kinase. J. Cell. Biochem., *77:* 333–344, 2000.

29. Birkenkamp, K. U., Dokter, W. H. A., Esselink, M. T., Jonk, L. J. C., Kruijer, W., and Vellenga, E. A dual function for p38 MAP kinase in hematopoietic cells: involvement in apoptosis and cell activation. Leukemia (Baltimore), *13:* 1037–1045, 2000.

30. Leppa, S., and Bohmann, D. Diverse functions of JNK signalling and c-Jun in stress response and apoptosis. Oncogene, *18:* 6158–6162, 1999.

31. Xue, L., Murray, J. H., and Tolkovsky, A. M. The Ras/phosphatidylinositol 3-kinase and Ras/ERK pathways function as independent survival modules each of which inhibits a distinct apoptotic signaling pathway in sympathetic neurons. J. Biol. Chem., *275:* 8817–8824, 2000.

32. Toker, A. Protein kinases as mediators of phosphoinositide 3-kinase signaling. Mol. Pharmacol., *57:* 652–658, 2000.

33. Datta, S. R., Brunet, A., and Greenberg, M. E. Cellular survival: a play in three Akts. Genes Dev., *13:* 2905–2927, 1999.

34. Vanhaesebroeck, B., and Alessi, D. R. The PI3K-PDK1 connection: more than just a road to PKB. Biochem. J., *346:* 561–576, 2000.

35. Cardone, M. H., Roy, N., Stennicke, H. R., Salvesen, G. S., Franke, T. F., Stanbridge, E., Frisch, S., and Reed, J. C. Regulation of cell death protease caspase-9 by phosphorylation. Science (Wash. DC), *282:* 1318–1321, 1998.

36. Brunet, A., Bonni, A., Zigmond, M. J., Lin, M. Z., Juo, P., Hu, L. S., Anderson, M. J., Arden, K. C., Blenis, J., and Greenberg, M. E. Akt promotes cell survival by phosphorylating and inhibiting a Forkhead transcription factor. Cell, *96:* 857–868, 1999.

37. Datta, S. R., Dudek, H., Tao, X., Masters, S., Fu, H., Gotoh, Y., and Greenberg, M. E. Akt phosphorylation of BAD couples survival signals to the cell-intrinsic death machinery. Cell, *91:* 231–241, 1997.

38. del Paso, L., Gonzalez-Garcia, M., Page, C., Herrera, R., and Nunez, G. Interleukin-3-induced phosphorylation of BAD through the protein kinase Akt. Science (Wash. DC), *278:* 687–689, 1997.

39. Tang, Y., Zhou, H., Chen, A., Pittman, R. N., and Field, J. The Akt proto-oncogene links Ras to Pak and cell survival signals. J. Biol. Chem., *275:* 9106–9109, 2000.

40. Zha, J., Harada, H., Yang, E., Jockel, J., and Korsmeyer, S. J. Serine phosphorylation of death agonist BAD in response to survival factor results in binding to 14-3-3 not BCL-X_L. Cell, *87:* 619–628, 1996.

41. Pugazhenthi, S., Nesterova, A., Sable, C., Heidenreich, K. A., Boxer, L. M., Heasley, L. E., and Reusch, J. E.-B. Akt/protein kinase B up-regulates Bcl-2 expression through cAMP-response element-binding protein. J. Biol. Chem., *275:* 10761–10766, 2000.

42. Madrid, L. V., Wang, C-Y., Guttridge, D. C., Schottelius, A. J. G., Baldwin, A. S., Jr., and Mayo, M. W. Akt suppresses apoptosis by stimulating the transactivation potential of the RelA/p65 subunit of NF-κB. Mol. Cell. Biol., *20:* 1626–1638, 2000.

43. Burow, M. E., Weldon, C. B., Melnik, L. I., Duong, B. N., Collins-Burow, B. M., Beckman, B. S., and McLachlan, J. A. PI3-K/AKT regulation of NF-κB signaling events in suppression of TNF-induced apoptosis. Biochem. Biophys. Res. Commun., *271:* 342–345, 2000.

44. Stambolic, V., Mak, T. W., and Woodgett, J. R. Modulation of cellular apoptotic potential: contributions to oncogenesis. Oncogene, *18:* 6094–6103, 1999.

45. Maehama, T., and Dixon, J. E. The tumor suppressor, PTEN/MMAC1, dephosphorylates the lipid second messenger, phosphatidylinositol 3,4,5-trisphosphate. J. Biol. Chem., *273:* 13375–13378, 1998.

46. Howells, L., Gallacher-Horley, B., Hudson, A., and Manson, M. M. Indole-3-carbinol inhibits PKB/Akt phosphorylation and induces apoptosis in a human breast tumor cell line. Proc. Am. Assoc. Cancer Res., *42:* 312, 2001.

47. Dampier, K. Mechanism of Action of the Chemopreventive Agent Genistein. Centre for Mechanisms of Human Toxicity (Thesis), pp. 83–84. Leicester, UK: University of Leicester, 2000.

48. Hudson, E. A., Dinh, P. A., Kokubun, T., Simmonds, M. S. J., and Gescher, A. Characterization of potentially chemopreventive phenols in extracts of brown rice that inhibit the growth of human breast and colon cancer cells. Cancer Epidemiol. Biomark. Prev., *9:* 1163–1170, 2000.

49. Staal, F. J. T., Roederer, M., and Herzenberg, L. A. Intracellular thiols regulate activation of nuclear factor κB and transcription of human immunodeficiency virus. Proc. Natl. Acad. Sci. USA, *87:* 9943–9947, 1990.

50. Plummer, S. M., Holloway, K. A., Manson, M. M., Munks, R. J. L., Kaptein, A., Farrow, S., and Howells, L. Inhibition of cyclo-oxygenase 2 expression in colon cells by the chemopreventive agent curcumin involves inhibition of NF-κB activation via the NIK/IKK signalling complex. Oncogene, *18:* 6013–6020, 1999.

51. Snedecor, G. W., and Cochran, W. G. Analysis of variance. *In:* G. W. Snedecor and W. G. Cochran (eds.), Statistical Methods, Ed. 7, pp. 215–237. Ames, IA: The Iowa State University Press, 1980.

52. Afifi, A. A., and Azen, S. P. The analysis of variance. *In:* A. A. Afifi and S. P. Azen (eds.), Statistical Analysis: A Computer-oriented Approach, Ed. 2, pp. 198–273. London: Academic Press, Inc., 1979.

53. Ozes, O. N., Mayo, L. D., Gustin, J. A., Pfeffer, S. R., Pfeffer, L. M., and Donner, D. B. NF-κB activation by tumour necrosis factor requires the Akt serine-threonine kinase. Nature (Lond.), *401:* 82–85, 1999.

54. Romashkova, J. A., and Makarov, S. S. NF-κB is a target of AKT in anti-apoptotic PDGF signalling. Nature (Lond.), *401:* 86–90, 1999.

55. Lu, Y., Lin, Y-Z., LaPushin, R., Cuevas, B., Fang, X., Yu, S. X., Davies, M. A., Khan, H., Furui, T., Mao, M., Zinner, R., Hung, M-C., Steck, P., Siminovitch, K., and Mills, G. B. The PTEN/MMAC1/TEP tumor suppressor gene decreases cell growth and induces apoptosis and anoikis in breast cancer cells. Oncogene, *18:* 7034–7045, 1999.

56. Nakatani, K., Thompson, D. A., Barthel, A., Sakaue, H., Liu, W., Weigel, R. J., and Roth, R. A. Up-regulation of Akt3 in estrogen receptor-deficient breast cancers and androgen-independent prostate cancer lines. J. Biol. Chem., *274:* 21528–21532, 1999.

57. Sheng, H. M., Shao, J. Y., and DuBois, R. N. Akt/PKB activity is required for Ha-Ras-mediated transformation of intestinal epithelial cells. J. Biol. Chem., *276:* 14498–14504, 2001.

58. Meng, Q. H., Goldberg, I. D., Rosen, E. M., and Fan, S. J. Inhibitory effects of indole-3-carbinol on invasion and migration in human breast cancer cells. Breast Cancer Res. Treat., *63:* 147–152, 2000.

59. Hsu, A-L., Ching, T-T., Wang, D-S., Song, X., Rangnekar, V. M., and Chen, C-S. The cyclooxygenase-2 inhibitor celecoxib induces apoptosis by blocking Akt activation in human prostate cancer cells independently of Bcl-2. J. Biol. Chem., *275:* 11397–11403, 2000.

60. Heiss, E., Herhaus, C., Klimo, K., Bartsch, H., and Gerhauser, C. Nuclear factor κB is a molecular target for sulforaphane-mediated anti-inflammatory mechanisms. J. Biol. Chem., *276:* 32008–32015, 2001.

61. Otsuki, M., Saito, H., Xu, X., Sumitani, S., Kouhara, H., Kurabayashi, M., and Kasayama, S. Cilostazol represses vascular cell adhesion molecule-1 gene transcription via inhibiting NF-κB binding to its recognition sequence. Atherosclerosis (Berlin), *158:* 121–128, 2001.

62. Cernuda-Morollon, E., Pineda-Molina, E., Canada, F. J., and Perez-Sala, D. 15-Deoxy-D-12,14-prostaglandin J2 inhibition of NF-κB-DNA binding through covalent modification of the p50 subunit. J. Biol. Chem., *276:* 35530–35536, 2001.

63. Heppner, C., Bilimoria, K. Y., Agarwal, S. K., Kester, M., Whitty, L. J., Guru, S. C., Chandrasekharappa, S. C., Collins, F. S., Spiegel, A. M., Marx, S. J., and Burns, A. L. The tumor suppressor protein menin interacts with NF-κB proteins and inhibits NF-κB-mediated transactivation. Oncogene, *20:* 4917–4925, 2001.

64. Haridas, V., Arntzen, C. J., and Gutterman, J. U. Avicins, a family of triterpenoid saponins from *Acacia victoriae* (Bentham), inhibit activation of nuclear factor-κB by inhibiting both its nuclear localization and ability to bind DNA. Proc. Natl. Acad. Sci. USA, *98:* 11557–11562, 2001.